



Science Arts & Métiers (SAM)

is an open access repository that collects the work of Arts et Métiers Institute of Technology researchers and makes it freely available over the web where possible.

This is an author-deposited version published in: <https://sam.ensam.eu>
Handle ID: <http://hdl.handle.net/10985/13274>

To cite this version :

Rémy FABBRO, Morgan DAL, Patrice PEYRE, Frédéric COSTE, Matthieu SCHNEIDER, V GUNENTHIRAM - Analysis and possible estimation of keyhole depths evolution, using laser operating parameters and material properties - Journal of Laser Applications - Vol. 30, p.Article number 032410 - 2018

Any correspondence concerning this service should be sent to the repository

Administrator : archiveouverte@ensam.eu



Analysis and possible estimation of keyhole depths evolution, using laser operating parameters and material properties

Remy Fabbro, Morgan Dal, Patrice Peyre, Frédéric Coste, Matthieu Schneider, and Valerie Gunenthiram

PIMM Laboratory, Ensam-Cnrs-Cnam, 151, Bd. De l'Hôpital, 75013 Paris, France

The authors propose an analysis of the effect of various operating parameters on the keyhole depth during laser welding. The authors have developed a model that uses the analysis of the thermal field obtained in 2D geometry, which is mainly defined by the characteristic Peclet number. This allows us to show that the dependence of the aspect ratio R of the keyhole with the operating parameters of the process is a function of two parameters: a normalized aspect ratio R_0 , controlled by the incident laser power and the spot diameter, and a characteristic speed V_0 related to the process of heat diffusion. The resulting general law $R = f(R_0, V/V_0)$ appears to be very well verified by different experimental data and allows to define mean thermophysical parameters of the used materials. These data can then be used for keyhole depths prediction for any subsequent operating parameters of the same material. This model also allows us to define precisely a criterion for a keyhole threshold generation. The authors will apply the derived procedure to successfully analyze experiments on materials with very different thermophysical properties (such as steel alloys and copper), with various focal spots, incident laser powers, and welding speeds.

Key words: laser welding, keyhole, keyhole depth estimation

I. INTRODUCTION

Laser beam welding in deep penetration mode, using a keyhole (KH) mode, is now a very attractive and popular process. Because of the possible wide range of laser operating parameters, KH depths ranging from a few hundred microns to several tens of millimeters can be easily produced in many different metallic materials. However, the predictability of these KH depths as a function of the operating parameters and the thermophysical properties of the used material is very far from being achieved. Specific experiments producing tables seem to be up to now the best way for obtaining reliable data. However, since almost 40 years, in connection with the growing knowledge of physical phenomena occurring during this type of interaction, many more or less complex models have been developed with variable satisfactory results. Following the pioneering work of Rosenthal,¹ many studies analyzed the thermal field induced by a line source² or a cylindrical KH (Refs. 3–7) moving inside the workpiece. Thereafter, numerical simulations were used and due to the increased computational capability and the improvement of numerical algorithms, much more physical processes could be added to achieve 3D complex numerical simulations describing the melt pool hydrodynamics, and taking into account free surfaces deformation, vapor and plasma effects, or multiple beam reflections inside the KH.^{8–14} However, it is clear that these complex numerical simulations can only be handled by skilled researchers and moreover, they are not practically realized in realistic frame time. If we are only interested in estimating the KH depth, with a satisfying precision for a given set of operating

parameters and materials, we need a much simpler method. By using an intermediate approach, initially proposed by Lankalapalli *et al.*,⁶ where a thermal analysis of this process coupled to the results of 2D simulations is used, we will show how this approach can be adapted to the analysis of different experimental results and then for estimating the KH depths for subsequent operating parameters.

In the first part of this paper, we will define a criterion for KH generation. Then, after the description of the thermal model and its improvement, we will discuss how it can be adapted to the KH depth analysis. Finally, we will discuss its application to several experimental situations concerning the welding of different materials.

II. THRESHOLD FOR KH GENERATION

During a laser welding process, a KH appears only if specific conditions on operating parameters are met. Figure 1 shows the transition of the melt pool to a KH geometry, when for example one varies the welding speed V , for a given incident power P . At high welding speed V , a melt pool appears when the surface temperature reaches the melting temperature T_m [Fig. 1(a)]. Then if the welding speed is decreased, the surface temperature reaches the evaporation one T_v , and the surface below the laser spot begins to be depressed by the recoil pressure [Fig. 1(b)], but the reflected incident beam is still reflected upwards, which carries away about typically 60% from the incident laser power (at $1.06\mu\text{m}$, on steel alloys¹⁵). By a further reduction of the welding speed, due to the resulting increase in surface

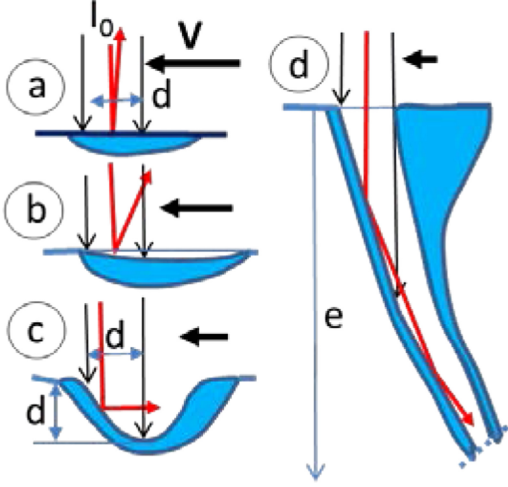


FIG. 1. (a–d) As a function of the welding speed V , evolution of the melt pool geometry leading to the KH formation.

temperature and the subsequent recoil pressure, the deformation of the melt pool surface increases and the inclination of what will be the KH front can reach 45° [Fig. 1(c)]; the reflected beam is then horizontal, and of course, any further reduction of the welding speed will make it to be directed downwards [Fig. 1(d)], adding its contribution to an increased penetration leading to a KH, where quite all the incident beam is trapped. Following this scheme, it is clear that the threshold for KH generation is defined by finding the conditions where the inclination angle of the KH front is about 45° , or equivalently, when the penetration depth e is equal to the laser spot diameter d : $e \approx d$.

For finding these conditions, we use a previous model that gives the KH front inclination angle and the penetration depth e resulting of the first impact of the laser beam.¹⁶ The corresponding penetration depth e is then given by

$$\frac{e}{d} \approx \frac{4A_0}{\pi H_0} \frac{P}{V \cdot d^2}, \quad (1)$$

where A_0 is the absorption coefficient under normal incidence, P is the incident power (W), and H_0 (in J/m^3) is the enthalpy necessary to the melting of the incoming solid. By using the ‘‘piston model,’’¹⁷ it is easy to show that for operating conditions where the evaporation process is negligible, $H_0 = h_m + h_s f(Pe)$, where $h_m = \rho_s [C_{ps}(T_m - T_0) + L_m + C_{pm}(T_v - T_m)/2]$ is a modified enthalpy at fusion [an average temperature $(T_m + T_v)/2$ of the sideways ejected liquid is considered], and $h_s = \rho_s C_{ps}(T_m - T_0)$ is the enthalpy at melting. The function $f(Pe) = uPe^{-\nu}$ defines the conduction losses, where $Pe = Vd/2k$ is the usual Peclet number (k : heat diffusivity), and the constants u and ν depend of the considered geometry [for example, $u \approx 2^{0.7}$ and $\nu = 0.7$, for a strip of width d (Ref. 18)].

With the condition $e = d$ in Eq. (1), it is then possible to define the threshold for KH formation which becomes:

$$\frac{P}{V \cdot d^2} = \frac{\pi H_0}{4 A_0}. \quad (2)$$

It is worth noticing that Eq. (2) can be rewritten as $A_0 P = (\pi d^2/4) \cdot V \cdot H_0$, which appears to be an energy balance equation defining the absorbed power $A_0 P$ required for delivering the heat enthalpy H_0 , to a volume rate $(\pi d^2/4) \cdot V$ of solid material ($\pi d^2/4 \approx d^2$ is the section of the incoming solid material) [see Fig. 1(c)]. The experimental validation of this threshold determination will be discussed at the end of Sec. III.

III. ESTIMATION OF THE KH DEPTH

The KH geometry used here is shown in Fig. 2. We assume a vertical cylindrical KH geometry, with its surface at the evaporation temperature T_v of the material and all the incident laser power P is homogeneously absorbed on the KH wall surface, along the KH depth e . Therefore, e verifies the relation $e = P/P_z$, where $P_z = dP/dz$ is the absorbed power per unit depth injected inside the KH necessary for maintaining the KH surface at T_v .

P_z can be determined by analyzing the resulting 2D-thermal field for this 2D geometry. If we assume constant thermophysical properties, no solid–liquid phase change, and a welding speed V along the x -direction, the 2D heat equation is then:¹

$$\rho C_p \frac{\partial T}{\partial t} + \rho C_p V \frac{\partial T}{\partial x} = K \left(\frac{\partial^2 T}{\partial x^2} + \frac{\partial^2 T}{\partial y^2} \right), \quad (3)$$

with $T = T_0$ at $x, y \rightarrow \pm\infty$, and $T = T_v$ for $r = (x^2 + y^2)^{1/2} = d/2$. (K : heat conductivity; C_p : heat capacity).

If one introduces the dimensionless variables:

$T' = T/(T_v - T_0)$, $x' = 2 \cdot x/d$, $y' = 2 \cdot y/d$, $t' = 2 \cdot t/d$ and $t' = t/\tau$ (with $\tau = d^2/4k$), then Eq. (3) becomes:

$$\frac{\partial T'}{\partial t'} + Pe \cdot \frac{\partial T'}{\partial x'} = \frac{\partial^2 T'}{\partial x'^2} + \frac{\partial^2 T'}{\partial y'^2}. \quad (4)$$

Equation (4) shows that the Peclet number Pe is the only parameter controlling the thermal field and its resulting gradient at the KH surface. Using Finite Element Modeling (FEM), it is easy to check that the stationary state is obtained for

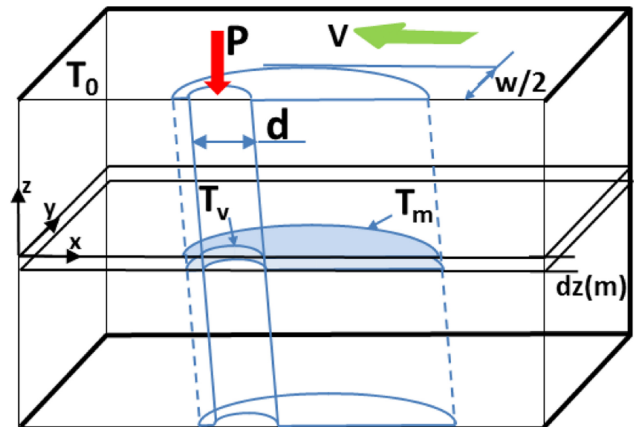


FIG. 2. Sketch of the longitudinal section of an inclined keyhole. The incident beam power is P . The KH surface is T_v and its diameter is d . The width of the melting isotherm T_m is w . Welding speed is V .

$r' \geq 3-4$. An analytical solution of this thermal field obtained in stationary conditions has already been derived using the polar coordinates (r, θ) .^{1,4-6,19} It can also be determined from 2D FEM calculation. We did here because it also allows us to consider the input laser power devoted to the solid–liquid phase change, which cannot be derived from the analytical solution of Eq. (4).

From the resulting thermal field, for stationary conditions, it is then possible to determine the input power P_z conducted through the KH surface:

$$\begin{aligned} P_z &= \int_0^{2\pi} -K \left(\frac{\partial T(r, \theta)}{\partial r} \right)_{r=d/2} r d\theta \\ &= K(T_v - T_0) \cdot \int_0^{2\pi} -K \left(\frac{\partial T'(r', \theta)}{\partial r'} \right)_{r'=1} d\theta \\ &= K(T_v - T_0) \cdot g(Pe). \end{aligned} \quad (5)$$

The function $g(Pe)$ has been plotted in Fig. 3. Equation (5) shows that as the welding speed (or the Peclet number) increases, the input power P_z at the KH surface, which is also dissipated from this zone by convection, must increase in order to keep a constant surface temperature of the KH at T_v .

Lankalapalli *et al.*⁶ have shown that $g(Pe)$, on the range $0 < Pe < 5$, could be approximated by an empirical equation expressed by a third degree polynomial expression. But in the present work, for the analysis of experimental results, we will see below the great interest of a very different approach: One uses a linear relation $g(Pe) = m \cdot Pe + n$ instead of the third degree polynomial expression.

But because of the non-linear behavior of $g(Pe)$, and in order to keep a good accuracy on $g(Pe)$ whatever the value of Pe (i.e., with a correlation index greater than 0.99), one must therefore use different linear relations defined by the pair (m, n) , along the Pe range. This means that the parameters m and n must vary with Pe . For $0.01 \leq Pe \leq 10$, we have defined five ranges of Pe , each having a variation dynamics of Pe of about 6, and for which the average value

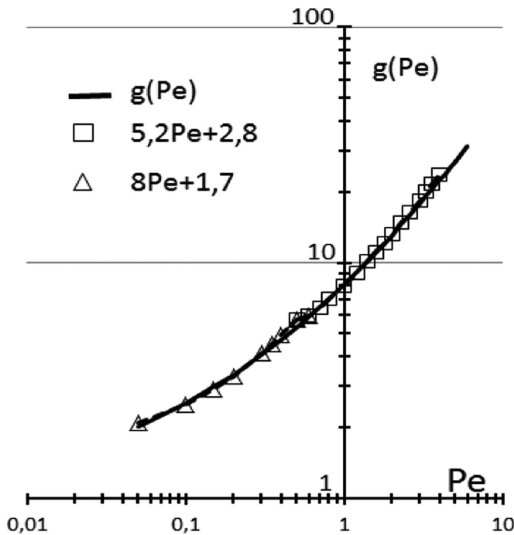


FIG. 3. Variation $g(Pe)$ as a function of the Peclet number Pe . Examples of two linear fits are shown.

of the pair (m, n) has been determined. The values of the pairs (m, n) on these five different ranges have been reported in Fig. 4. It is worth recalling that most of the experiments usually realized on steels have corresponding Peclet numbers in the range $0.2 < Pe < 6$, where typically $m \approx 5$ and $n \approx 3$. Two examples of these linear fits have been also reported in Fig. 3.

We have now all the elements for determining the aspect ratio $R = e/d$. Using Eq. (5), one can write:

$$\begin{aligned} R &= \frac{e}{d} = \frac{P}{d \cdot P_z} = \frac{P}{d \cdot K \cdot (T_v - T_0) \cdot g(Pe)} \\ &= \frac{P}{d \cdot K \cdot (T_v - T_0) \cdot (m \cdot Pe + n)}. \end{aligned} \quad (6)$$

As $Pe = V \cdot d / 2 \cdot \kappa$, Eq. (6) can be rewritten in a much-generalized form:

$$R = \frac{R_0}{(1 + V/V_0)}, \quad (7a)$$

with

$$R_0 = \frac{P}{n \cdot d \cdot K \cdot (T_v - T_0)} \text{ and } V_0 = 2 \frac{n \cdot k}{m \cdot d}. \quad (7b)$$

The interest of the very simple Eq. (7a) is that it gives the scaling law of the KH depth with all the parameters of this problem. Moreover, it reproduces the variations of the KH depth e that are usually observed experimentally: at high welding speeds (if $V \gg V_0$, V_0 being characteristic of some “speed” of heat diffusion), one finds $R \approx R_0 \cdot V_0 / V$, and it is known that at high welding speeds, the KH depth e is roughly inversely proportional to the welding speed V . On the contrary, when the welding speed decreases, (or $V < V_0$), it is observed that the penetration depth e increases and then saturates. Equation (7) reproduces this behavior and the maximum aspect ratio is then equal to R_0 . These trends can

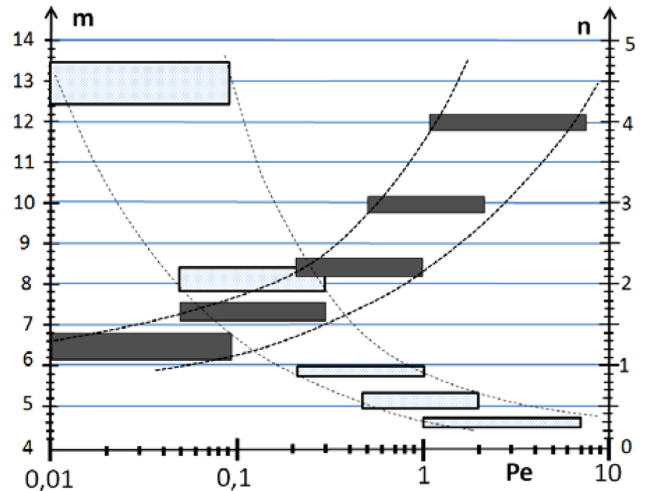


FIG. 4. Inside five selected Pe intervals, ranging from $Pe = 0.01$ to $Pe = 10$, mean values of the pair of parameters m (empty symbols) and n (filled symbols) used for defining the corresponding best fit for a linear variation of $g(Pe)$, as $g(Pe) = mPe + n$.

be understood by considering the ratio convection/conduction losses that are of course directly related to the Peclet number: at low Pe (or low V), convection becomes negligible (and even null for $V=0$); the input power P_z inside the KH is small and so the incident laser power P can be distributed on a greater (and maximum) depth. At high Pe (or high V), convection dominates and makes P_z to increase quite linearly with the welding speed: the penetration depth then decreases.

Remark 1: From Eq. (7), one sees that the aspect ratio R depends on two operating parameters: P/d and V . But Eq. (7a) can also be rewritten as

$$R = \frac{P/Vd^2}{\Delta H_v} \cdot \frac{1}{(1 + V_0/V)}, \quad (8)$$

with

$$\Delta H_v = 0.5m\rho C_p(T_v - T_0). \quad (8a)$$

In that case, one can see that R is mainly defined by the ratio of two volumetric energy densities (in J/m^3): P/Vd^2 is related to the operating parameters, and ΔH_v to the thermophysical properties of the material, which is a kind of enthalpy parameter that contains the evaporation temperature T_v . Moreover, using Eq. (8), one can find that the threshold for KH generation, i.e.: $R \geq 1$, is defined by

$$\frac{P}{Vd^2} \geq \frac{\Delta H_v}{A_0}. \quad (9)$$

In Eq. (9), when $R=1$, we must take into account the absorptivity of the incident beam for these conditions, which is near A_0 , and not quite 100% as in the case of deep penetration when a large beam trapping occurs. More rigorously, in Eq. (7) or (8), one should also take into account the level of absorptivity of the incident laser beam, which is defined by the number of multiple reflections inside the KH that depends on the aspect ratio R . It is known that this absorptivity increases from A_0 to nearly 100% when the aspect ratio R increases from 0 to about 8–10, due to increased beam trapping efficiency.^{20,21} It is also interesting to notice that the two KH thresholds defined by Eqs. (9) and (2) have the same order of magnitude, although obtained with very different approaches [see Eqs. (2) and (9)]. Indeed, it is found that $\Delta H_v/H_0 \approx 3$ (thermophysical parameters of SS304 L were used).

Remark 2: Equation (8) can also be rewritten as an energy balance equation: $A_0 \cdot P = V \cdot (e \cdot d) \cdot \Delta H_v \cdot (1 + V_0/V)$ that gives a more physical interpretation of the obtained law. At high welding speed, $A_0 \cdot P$ is the absorbed power necessary to give to the volume rate $V \cdot (e \cdot d)$ of solid material ($e \cdot d$ being the section of incoming solid material), the enthalpy ΔH_v that contains information on both the heating from T_0 to T_v and the overall heat diffusion process through the parameter m .

Remark 3: The scaling of the KH depths [Eq. (7)] with the thermophysical parameters shows that the KH depth increases with reduced heat conductivities K or with low evaporation temperatures T_v . This is in agreement with the observed increase in the KH depth due to the decrease in T_v as a result, for example, of welding under reduced ambient pressure.²²

IV. EFFECT OF SOLID–LIQUID PHASE CHANGE

The previous analysis has determined the heat input inside the KH without considering any solid–liquid phase change that generates the observed liquid melt pool during laser welding. It is therefore important to estimate the power that is necessary to add to the incident one previously determined, for this melt pool generation. In Fig. 2, one can see that the only part of the solid material that undergoes this phase change is located between $y = \pm w/2$ (w being the width of the isotherm at T_m). As this part already undergoes the heating from T_0 to T_m , its subsequent melting requires only the enthalpy of fusion L_m . Therefore, as the material is flowing at the welding speed V , the excess of incident power (per unit depth) ΔP_z^m necessary for this process is given by

$$\Delta P_z^m = V w \rho L_m. \quad (10)$$

For evaluating ΔP_z^m , the width w of the melting isotherm must be known. Beck²¹ has proposed an analytical approximation for w/d :

$$w/d = 1 + G(T_v, T_m, T_0) Pe^{-0.5}, \quad (11)$$

where

$$G(T_v, T_m, T_0) = 2^{3.5} \left(\frac{T_v - T_m}{T_v + T_m - 2T_0} \right)^2. \quad (12)$$

By using the FEM COMSOL software,²³ we have verified the validity of Eq. (11), for the Peclet range $0.08 < Pe < 10$. In order to quantify the importance of this excess of power ΔP_z^m , we have to compare it with the previously determined input power P_z :

$$\begin{aligned} \Delta P_z^m &= \frac{V d \rho L_m (w/d)}{K(T_v - T_0) (mPe + n)} \\ &= 2 \frac{L_m}{C_p(T_v - T_0)} \left(\frac{Pe(1 + GPe^{-0.5})}{mPe + n} \right). \end{aligned} \quad (13)$$

As typically $2 \cdot L_m / (C_p \cdot (T_v - T_0)) \approx 0.40$, it can be seen that the ratio $\Delta P_z^m / P_z$ varies from 0, at low Pe (or low welding speeds), to $\approx 0.40/m \approx 8.5\%$ at high welding speeds. Therefore, the power required to achieve this phase change is less than 10% of the input power used in the generation of the entire thermal field inside the workpiece. So, we will neglect this effect for the analysis of the experimental results described in Sec. V.

V. APPLICATION TO THE ANALYSIS OF EXPERIMENTS

The expression of the KH aspect ratio R according to Eq. (7a) is very interesting, because it shows that $1/R$ becomes a linear function of the welding speed V . Indeed, we see that

$$\frac{1}{R} = \frac{1}{R_0} \left(1 + \frac{V}{V_0} \right) = \frac{V}{R_0 V_0} + \frac{1}{R_0} = aV + b. \quad (14)$$

So, for a given set of experimental results, if one plots $1/R$ as a function of the welding speed V , one should find a linear function whose slope is a and the ordinate at the origin, b . Knowing a and b , from Eq. (14), one can then determine easily R_0 and V_0 from:

$$R_0 = \frac{1}{b} \quad \text{and} \quad V_0 = \frac{b}{a}. \quad (15)$$

It is this procedure that we have applied below to several experiments realized with different operating parameters or materials. The interest of this method is that it uses a fit of experimental data to define the parameters R_0 and V_0 , and not Eq. (7b), which requires the knowledge of average values of K and k , which are always difficult to define because of their strong dependence with temperature. Once R_0 and V_0 are estimated with this procedure, for example, for a given set of initial experiments, one can use them for predicting the KH depths for other operating parameters, for the same material.

Of course, by using directly Eqs. (7a) and (7b) with some “assumed” parameters for K and k , one may have some initial estimate of the KH depths, which may be very useful for preliminary experiments.

A. Analysis of several experiments

We first applied here our procedure for the analysis of recently published data on KH depths obtained on St35 steel at $1.06\ \mu\text{m}$ laser wavelength for different incident laser powers and focal spots.²⁴

In Fig. 5, the inverse of the aspect ratio $1/R$ has been plotted, as a function of the welding speed, for the three incident laser powers: 2, 5, and 8 kW, and two focal spot diameters: 0.78 and 0.38 mm, used by Suder and Williams.²⁴ The corresponding best linear fits for these data are also shown.

As in Fig. 5, we have plotted in Fig. 6 the variation of $1/R$ as a function of welding speed, for different laser powers and focal spot diameters when laser welding of copper in deep penetration mode, from experiments of Heider *et al.*²⁵

Due to the rather important uncertainties for determining KH depths at high welding speeds from the data collected

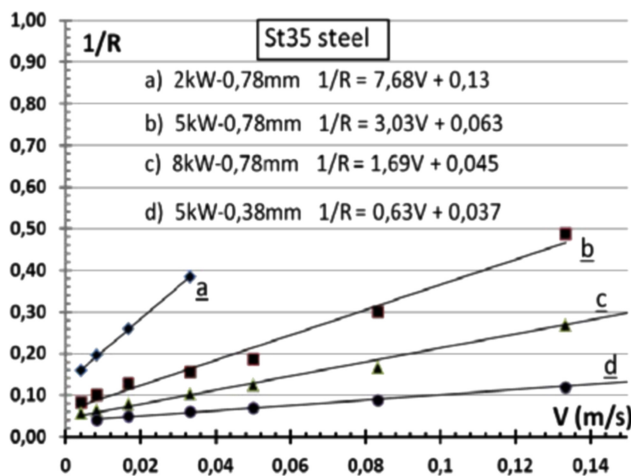


FIG. 5. For St35 steel and different operating parameters, plot of $1/R$ as a function of the welding speed V and corresponding best linear fits.

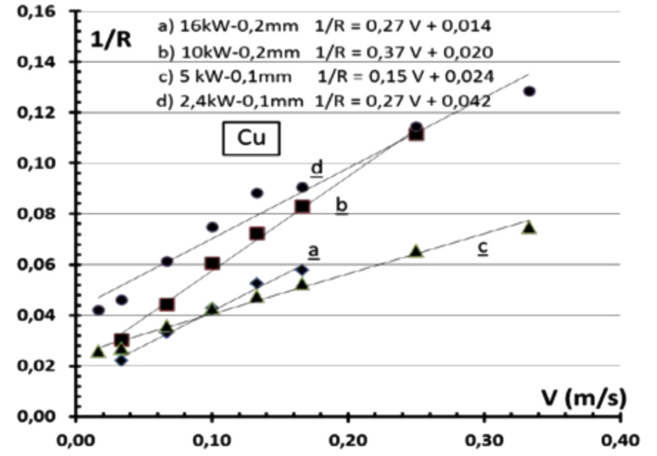


FIG. 6. For Cu and different operating parameters, plot of $1/R$ as a function of the welding speed V and corresponding best linear fits.

from Refs. 24, 25, only data for $R \geq 3$ have been reported in Figs. 5 and 6. Moreover, a high aspect ratio also should ensure a large trapping of the incident laser beam inside the KH,^{20,21} and so less uncertainty on the beam absorptivity, which is quite 100%, as well as a better 2D induced thermal field, which is one of the main constraints of our thermal model. For all these different experiments, one must notice the remarkable linear dependence of $1/R$ with the welding speed V .

B. Discussion

From the slope a , and the ordinate at origin b for each linear fit, and then using Eq. (15), the parameters R_0 and V_0 entering in Eq. (7a) have been determined.

For both materials, their values have been reported in Table I (with the label “fit”), and can be compared with those expected when Eq. (7b) is estimated (label “direct”) by using mean thermophysical data at melting temperature²⁶ and the m and n parameters derived from Fig. 4 on the corresponding Pe range of these experiments.

In Table I, the parameters V_0 and R_0 derived from the linear fits and those estimated from assumed mean values of K and k are rather close and similarly follow the expected tendencies: R_{0F} increases with the incident laser power and with a decrease in the focal spot diameter. For the St35 steel, the mean “diffusion” velocity V_{0F} of about 0.022 m/s for the 0.78 mm experiments is doubled when the spot diameter decreases to 0.38 mm. From the V_{0F} variations, on Cu experiments compared to the steel experiments, one can also see that our model catches fairly well the great difference of heat diffusivity and spot sizes between these two materials.

However, one can see that there are some differences between the “fitted” and “direct” parameters R_0 and V_0 . This results mainly from the choice of the selected parameters K and k that are rather arbitrary, and also, in the case of the parameter R_{0D} , from some possible overestimation of the absorbed power P . One knows that absorptions of about 80% of the incident laser power are usually considered, even inside large aspect ratio KH. In Table I, one can remark that the R_{0D} is always greater than the “fitted” one. By applying some reduction of about 80% to the incident power, both values

TABLE I. Parameters V_0 and R_0 from analysis of experiments (Refs. 24, 25).

	Material: St35 steel				Material: Cu			
Incident laser power (kW)	2	5	8	5	16	10	5	2.4
Spot diameter (mm)	0.78	0.78	0.78	0.38	0.2	0.2	0.1	0.1
V_{0F} (m/s) (from fit)	0.017	0.021	0.027	0.059	0.05	0.06	0.16	0.15
V_{0D} (m/s) (direct)	0.013	0.013	0.013	0.028	0.086	0.086	0.17	0.17
R_{0F} (from fit)	7.7	15.9	22.2	27.0	69.4	48.8	40.5	23.5
R_{0D} (direct)	7.6	19.0	30.5	39.1	84.1	52.6	52.6	25.2
Used parameters	$K \approx 30$ W/m·K, $k \approx 6 \cdot 10^{-5}$ m ² /s (Ref. 26) as $0.15 \leq Pe \leq 5$, $m \approx 4.5$ and $n \approx 4$				$K \approx 250$ W/m·K, $k \approx 6 \cdot 10^{-5}$ m ² /s (ref. 26) as $0.02 \leq Pe \leq 0.2$, $m \approx 10$ and $n \approx 1.5$			

would be much closer. Furthermore, once the Pe range is given, the parameters m and n are well enough defined (from Fig. 4); so, one then could estimate mean values of K and k from the R_{0F} and V_{0F} parameters. In doing so to the present results, one finds that the resulting mean values of K and k are slightly different from the assumed ones and they can be considered to be more representative of the mean thermophysical properties of this material for these welding conditions.

C. KH depth estimation procedure

The confidence resulting from the previous analysis allows us to propose a rather simple methodology for a rapid and easy KH depth estimation that can be described by the following steps:

- For a given material (that defines T_v , and mean values of K and k defined at fusion temperature of this material) and the set of operating parameters (incident laser power P , range of welding speeds V , spot diameter d), one first estimates the corresponding Pe range and therefore the corresponding parameters m and n to be used, from Fig. 4 for this Pe range.
- From these data, the parameters R_{0D} and V_{0D} , from Eq. (7b), and finally the variation of the aspect ratio R (or the KH depth) can be computed on this welding speed range [from Eq. (7a)].

However, if some experiments can be realized with these conditions (typically three different welding speeds are enough), the corresponding parameters R_{0F} and V_{0F} can be determined from the resulting linear plot of $1/R$ with the welding speed V . For other operating parameters on the same material, R_0 and V_0 will then be easily extrapolated from the previously determined R_{0F} and V_{0F} , by using their scaling laws from Eq. (7b) [where $V_{0D} \propto d^{-1}$ and $R_{0D} \propto (P/d)$].

This procedure can be tested with some results from Table I. Let us suppose that we have made some trials on St35 steel, at 5 kW with the 0.78 mm focal spot. From Table I, one sees that one would obtain $R_0 \approx 15.9$ and $V_0 \approx 0.013$ m/s. If one uses these data for estimating R_0 for experiments that would be realized at 8 kW with the same focal spot, one finds that $R_0 \approx 15.9(8/5) = 25.4$, which is about 13% greater than the experimental value of 22.2 given in Table I for these operating conditions. For experiments that would be realized at 5 kW with a 0.38 mm focal spot, one would obtain: $R_0 \approx 15.9(0.78/0.38) = 32.6$, which is about

17% greater than the corresponding experimental value of 27. This procedure can be applied to other operating conditions used in Table I and one finds that maximum typical differences of 20% can be seen between estimated and corresponding experimental values for R_0 .

So ultimately, one can see that the observed linear dependence of $1/R$ with the welding speed is very fruitful. One can add that this linear scaling can be observed in quite all the experiments dealing with laser welding in KH mode with high aspect ratios.

VI. CONCLUSION

We have extended the Lankalapalli *et al.*⁶ approach in order to define a model that contains more physical insights and an easier analysis of the relevant parameters from experimental data. This rather simple model allows a rapid and easy estimation of the KH depth as a function of the operating parameters (incident laser power, focal spot diameter, welding speed) and thermophysical parameters of the used material, for experiments performed at 1.06 μ m laser wavelength. Based on the assumption of a homogeneous deposition of incident laser power along the walls of a vertical cylindrical KH at evaporation temperature, this model gives the resulting final aspect ratio R as a function of the welding speed V , $R = R_0/(1 + V/V_0)$, which depends on two parameters: R_0 represents the maximum aspect ratio obtained when the welding speed V is zero, and a welding speed V_0 characteristic of the transition from conduction to convection dominated losses as the welding speed increases.

As this model shows that R^{-1} is a linear function of the welding speed V , which is consistent with the experiments, both parameters R_0 and V_0 can then be easily determined from few experiments. Once R_0 and V_0 are determined for specific operating parameters, they can be adapted for any other operating conditions of incident laser power, focal spot or welding speed for the same material. Of course, one can use this model in a direct approach by assuming ‘‘mean’’ thermophysical parameters defined at melting temperature, whose choice is a usually well-known difficulty when dealing with simplified thermal models. But in any case, these two approaches seem quite satisfactory; the linear scaling of R^{-1} with the welding speed is well verified and should be useful for different purposes such as the preparation or the analysis of experiments, or its use for some process control scheme.

- ¹D. Rosenthal, "The theory of moving sources of heat and its application to metal treatments," *Trans. ASME* **68**, 849–866 (1946).
- ²D. T. Swift-Hook and A. E. F. Gick, "Penetration welding with lasers," *Weld. Res. Suppl. J.* **52**, 492–499 (1973).
- ³J. Dowden, N. Postacioglu, M. Davis, and P. Kapadia, "A keyhole model in penetration welding with a laser," *J. Phys. D Appl. Phys.* **20**, 36–44 (1987).
- ⁴F. Noller, in *Proceedings of 3rd CISFFEL, International Colloquium on Welding and Melting by Electrons and Laser Beam* (Lyon, France, 1983), pp. 89–97.
- ⁵J. Kroos, U. Gratzke, and G. Simon, "Towards a self-consistent model of the keyhole in penetration laser beam welding," *J. Phys. D Appl. Phys.* **26**, 474–480 (1993).
- ⁶K. N. Lankalapalli, J. F. Tu, and M. Gartner, "A model for estimating penetration depth of laser welding processes," *J. Phys. D Appl. Phys.* **29**, 1831–1841 (1996).
- ⁷A. Kaplan, "A model of deep penetration laser welding based on calculation of the keyhole profile," *J. Phys. D Appl. Phys.* **27**, 1805–1814 (1994).
- ⁸D. Sudnik, D. Radaj, and W. Erofeew, "Computerized simulation of laser beam welding, modelling and verification," *J. Phys. D Appl. Phys.* **29**, 2811–2817 (1996).
- ⁹H. Ki, P. S. Mohanty, and J. Mazumder, "Modeling of laser keyhole welding: Part I. Mathematical modeling, numerical methodology, role of recoil pressure, multiple reflections, and free surface evolution," *Metall. Mater. Trans. A* **33**, 1817–1830 (2002).
- ¹⁰M. Geiger, K. H. Leitz, H. Koch, and A. Otto, "A 3D transient model of keyhole and melt pool dynamics in laser beam welding applied to the joining of zinc coated sheets," *Prod. Eng.* **3**, 127–36 (2009).
- ¹¹S. Pang, L. Chen, J. Zhou, Y. Yin, and T. Chen, "A three-dimensional sharp interface model for self-consistent keyhole and weld pool dynamics in deep penetration laser welding," *J. Phys. D Appl. Phys.* **44**, 025301 (2011).
- ¹²M. Courtois, M. Carin, P. Masson, S. Gaied, and M. Balabane, "A new approach to compute multi-reflections of laser beam in a keyhole for heat transfer and fluid flow modelling in laser welding," *J. Phys. D Appl. Phys.* **46**, 505305 (2013).
- ¹³W. Tan and Y. C. Shin, "Analysis of multi-phase interaction and its effects on keyhole dynamics with a multi-physics numerical model," *J. Phys. D: Appl. Phys.* **47**, 345501 (2014).
- ¹⁴H. Zhao, W. Niu, B. Zhang, Y. Lei, M. Kodoma, and T. Ishide, "Modelling of keyhole dynamics and porosity formation considering the adaptive keyhole shape and three-phase coupling during deep-penetration laser welding," *J. Phys. D: Appl. Phys.* **40**, 5753–66 (2011).
- ¹⁵M. Schneider, L. Berthe, R. Fabbro, and M. Muller, "Measurement of laser absorptivity for operating parameters characteristic of laser drilling regime," *J. Phys. D: Appl. Phys.* **41**, 155502 (2008).
- ¹⁶R. Fabbro, "Melt pool and keyhole behavior analysis for deep penetration laser welding," *J. Phys. D Appl. Phys.* **43**, 445501 (2010).
- ¹⁷V. Semak and A. Matsunawa, "The role of recoil pressure in energy balance during laser materials processing," *J. Phys. D Appl. Phys.* **30**, 2541–2552 (1997).
- ¹⁸W. Schulzt, D. Beckert, J. Franket, A. Kemmerlingt, and G. Herzigert, "Heat conduction losses in laser cutting of metals," *J. Phys. D Appl. Phys.* **26**, 1357–1363 (1993).
- ¹⁹H. S. Carslaw and J. C. Jaeger, *Conduction of Heat in Solids*, 2nd ed. (Clarendon, Oxford, 1962).
- ²⁰A. Gouffe, "Correction d'ouverture des corps noirs artificiels compte tenu des diffusions multiples internes," *Revue d'Optique* **24**, 1–10 (1945).
- ²¹M. Beck, "Modellierung des Lasertiefschweissens," Ph.D. Thesis, University of Stuttgart, Germany, 1996.
- ²²R. Fabbro, K. Hirano, and S. Pang, "Analysis of the physical processes occurring during deep penetration laser welding under reduced pressure," *J. Laser App.* **28**, 022427 (2016).
- ²³See <https://www.comsol.com>
- ²⁴W. J. Suder and S. Williams, "Power factor model for selection of welding parameters for CW laser welding," *Opt. Laser Technol.* **56**, 223–229 (2014).

²⁵A. Heider, P. Stritt, R. Weber, and T. Graf, in *Proceedings of ICALEO Conference* (San Diego, USA, 2014), pp. 343–348.

²⁶K. C. Mills, *Recommended Values of Thermophysical Properties for Selected Commercial Alloys* (Woodhead Publishing Limited, Abington Cambridge, England, 2002).

Meet the authors

Remy Fabbro is presently Emeritus Research Director at CNRS. His scientific career has always been devoted with laser–matter interaction, and since 1989, he is involved in the study of fundamental processes about industrial lasers applications, concerning laser welding and cutting processes (laser interaction, hydrodynamics, plasma, modeling, ...), and laser-shock processing (modeling of confined interaction mode, shock wave characterization, surface treatment). He published more than 120 papers in international journals and about 200 conference proceedings.

Morgan Dal is Associate Professor at PIMM laboratory at the Arts et Métiers Engineering School. Its research fields are mainly devoted to the numerical simulation of different laser applications, such as laser welding, additive manufacturing, or surface treatment. Since few years, in order to improve simulation efficiency, he is also studying the measurement of thermal properties of metals with the help of laser.

Patrice Peyre is a Research Director at CNRS. He has been working on materials transformation with lasers for 25 years. He has published more than 60 scientific papers on various topics (laser-shock peening, dissimilar welding, additive manufacturing). He is currently in charge of additive layer additive manufacturing activities in PIMM laboratory.

Frédéric Coste is working on laser applications since 1990, mainly on high thickness welding of carbon and stainless steel, laser–matter interaction instrumentation and laser surface treatment. Since 2009, he is in charge of the laser workshop at PIMM laboratory, in the Arts et Métiers ParisTech school. His main interest is now on the study of metallic pool under neutral and reactive gazes, and additive manufacturing.

Matthieu Schneider received his PhD in 2006. He has over 30 publications in peer-reviewed journals and conference proceedings and two patents related to laser processing and photonic science. He is an Associate Professor at the Arts et Métiers Engineering School and a member of the LIA. He is in charge of the Mechanical Engineering Semestre. His Research deals with laser processing (cutting, welding, drilling, and additive manufacturing).

Valerie Gunenthiram is a PhD student at the PIMM laboratory (Arts et Métiers ParisTech Engineering School, Paris), is currently studying the various phenomena that occur in selective laser melting, more specifically the laser–powder–melt pool interaction and related processes controlling the hydrodynamics of these melt pools and their consequences on the porosity origin.